AN ABSTRACT OF THE THESIS OF

Joseph J. McVeety for the degree of Master of Science in Electrical and Computer Engineering presented on August 13, 1999. Title: Analysis of Planar Multi-Conductor Multilayered Structures by Network Analog Method.

Abstract approved: Vijai K. Tripathi/Andreas Weisshaar

In this thesis the network analog method is used to analyze various planar multi-conductor structures in multilayered, lossy dielectric media. The method is based on an efficient impedance network representation of the finite difference approximation of Laplace's equation for the electric potential. Using the network analog method, the transmission line parameters are computed for several different uniform stripline structures in lossless and lossy multilayered dielectric material. The network analog method is also applied to several three-dimensional structures consisting of single and coupled conducting patches of rectangular shape. Results obtained with the network

analog method for single conducting patches in single and multilayered lossless dielectric media are in good agreement with published results based on a variational approach. Further results presented in this thesis include the coupling capacitance for coplanar and multilevel patch configurations in lossless and lossy multilayered dielectric media.

Analysis of Planar Multi-Conductor Multilayered Structures by Network Analog Method

by

Joseph J. McVeety

A THESIS

Submitted to

Oregon State University

in partial fulfillment of
the requirements for the
degree of

Master of Science

Presented August 13, 1999
Commencement June 2000

Master of Science thesis of Joseph J. McVeety presented

on August 13, 1999

APPROVED:

Redacted for Privacy

Co-Major Professor, representing Electrical and Computer Engineering

Redacted for Privacy

Co-Major Professor, representing Electrical and Computer Engineering

Redacted for Privacy

Head of Department of Electrical and Computer Engineering

Redacted for Privacy

Dean of Graduate School

I understand that my thesis will become part of the permanent collection of Oregon State University libraries. My signature below authorizes release of my thesis to any reader upon request.

Redacted for Privacy

Joseph J. McVeety, Author

ACKNOWLEDGEMENTS

I wish to gratefully acknowledge the assistance and support first and foremost of Dr. Vijai Tripathi. It is his work upon which this thesis is based and without whose help and encouragement I would not have finished. Attending Oregon State University during his tenure was a great privilege for me and he is someone I will always remember.

I also wish to deeply thank Dr. Andreas Weisshaar. He has also been a very big influence and guide in my studies at OSU. He has helped me to finally get to where I am and without his help I would not have been able to finish my studies.

Finally, I wish to acknowledge the help of Dr. Alok Tripathi. It was his inspiration which finally allowed me to unravel the mystery of this technique which had held me up for so long.

TABLE OF CONTENTS

LIST OF FIGURES

LIST OF FIGURES (Continued)

To Janice, Matthew and Amy....

Analysis of Planar Multi-Conductor Multilayered Structures by Network Analog Method

1. INTRODUCTION

Planar conducting structures, such as interconnects and pads, are used extensively in RF/microwave and digital circuits, both at the board level and on chip. In these circuits, the conducting structures often are embedded in multilayered dielectric media, which can be lossy. Examples include multilayered printed circuit boards and silicon integrated circuits. These types of structures are used in many different configurations and applications, and the understanding of their performance characteristics is essential to their successful design and implementation.

At low frequencies, the planar conducting structures can be accurately analyzed using quasi-static electromagnetic techniques. Quasi-static techniques typically are computationally much more efficient compared to full wave techniques, and the quasi-static solutions are usually sufficiently

accurate up to several gigahertz. From the electromagnetic analysis of a planar conducting structure, the values of appropriate circuit parameters characterizing the structure are then determined. For uniform interconnects (transmission lines) the circuit parameters are given, for example, in terms of distributed inductance and capacitance, whereas for single and coupled conducting patches, the self- and mutual capacitances are of interest.

In general, no rigorous closed-form solutions are available for many of the planar conducting structures. Over the years, many quasi-static and full wave electromagnetic techniques have been developed and applied to analyze these structures in order to determine the appropriate circuit parameters values that describe these structures. Each of these techniques can be applied with a mixture of accuracy, speed and versatility. In [1], a technique for solving an integral equation for the fields existing in the slots of a coplanar waveguide transmission system is presented. Tsai and De Flaviis [2] proposed a full-wave spatial domain analysis in which a dyadic Green's function is derived. Other methods include a spectral

domain approach [3], a vector finite element method [4], and full wave analysis [5], among many others.

The approach used here is the network analog method for determining the transmission line parameters of uniform interconnect structures and the coupling properties of planar conducting patches in multilayered, lossy dielectric media. The network analog method is a quasi-static technique that solves the finite difference approximation of the Laplace equation by transforming the electrostatic problem into a corresponding network problem. In addition to being computationally efficient, the network analog approach is an accurate and versatile method for determining the capacitance matrix of multi-conductor, multilayered structures with lossless or lossy media. For uniform coupled transmission lines, the capacitance matrix can also be used to determine the distributed inductance parameters, as will be shown in the following chapter.

The computation of the capacitance matrix for a uniform multi-conductor system for multilayered structures using a combination of multiport network theory and the finite-difference technique was presented by Lennartsson [6]. This technique allows for

a fast and accurate determination of the capacitance matrix for multiple zero thickness strips in two dimensions. Tripathi and Bucolo [7] expanded on this original technique to allow for the analysis of general lossy, anisotropic, multilayered structures including finite thickness strips on multiple levels. However, similar to Lennartsson's technique, this method is limited to two-dimensional structures. The additional theory to compute the coupling capacitance for three-dimensional strips was outlined in the appendix of another paper by Tripathi and Bucolo [8]. The expansion by Tripathi and Bucolo of the network analog method in [3] allows for efficient and accurate computation of the desired circuit parameters for lossy, multilayered structures with multiple conductors having finite width and length.

This thesis describes the implementation and application of the general three-dimensional network analog method for determining the capacitance matrix of multi-conductor multilevel structures in multilayered lossless and lossy dielectric media. Chapter 2 starts with the derivation of the electromagnetic equations for the stripline and microstrip for the very simple

case of a single conductor in a simple medium in order to demonstrate the complexity of problem. This analysis for even the simplest structures demonstrates the usefulness of techniques such as the network analog method. Further, it will be shown how the distributed inductance parameters for uniform transmission lines can be derived from the distributed capacitance and how lossy materials are included in the quasi-static approach.

Chapter 3 shows the derivation of the three-dimensional network analog method. Starting with simple network theory and progressing to the final matrix equations, all the equations for determining the capacitance matrix using this method will be derived. Also, the processing considerations necessary to make this technique efficient and accurate will be discussed.

In Chapter 4, the network analog method is evaluated and applied to various two- and three-dimensional structures with both single and multiple conductors in lossless and lossy dielectric media. First, the three-dimensional implementation of the network analog method is compared to a well-established

two-dimensional implementation of the method by analyzing several uniform transmission line structures. This comparison helps to set some processing time benchmarks, as well as verify the accuracy of the implemented code. In the following section, results obtained with the network analog method for single rectangular conducting patch structures in several multilayered dielectric configurations are compared to the published results. This comparison demonstrates the accuracy of the network analog method in analyzing three-dimensional conducting structures and further demonstrates its versatility and computational efficiency. Using the three-dimensional network analog method, the coupling characteristics of coupled rectangular patches in multilayered lossless and lossy dielectric media are examined.

Finally, conclusions and suggestions for further research are presented in Chapter 5.

2. QUASI-STATIC ANALYSIS

Single and multi-conductor structures in multi-layered lossy dielectric media can be analyzed by quasi-static methods at low frequencies, typically with accurate results obtained up to several gigahertz. For the electric potential Φ the three-dimensional Laplace equation is

$$\nabla^2\Phi = \left(\frac{\partial^2}{\partial x^2} + \frac{\partial^2}{\partial y^2} + \frac{\partial^2}{\partial z^2}\right)\Phi(x, y, z) = 0 . \qquad (2.1)$$

The solution is found in each homogenous dielectric layer subject to the boundary conditions with the conductor and at each interface between layers. Once Φ is known everywhere, the capacitance matrix (self and mutual capacitances) of the multi-conductor system can be obtained.

If lossy dielectric materials are present, the dielectric media can be characterized in terms of a complex permittivity

$$\tilde{\varepsilon} = \varepsilon' - j\varepsilon'' = \varepsilon' - j\frac{\sigma}{\omega} \qquad (2.2)$$

where σ is the conductivity of the medium. Then, computed capacitance is complex and given by

$$\tilde{C} = C - j\frac{G}{\omega}. \tag{2.3}$$

The conductance can thus be obtained from the imaginary part of the complex capacitance.

If the transmission line structure is uniform, the problem reduces to two dimensions. In other words, the problem becomes one of solving the two-dimensional Laplace equation in a cross-sectional plane of the structure. Uniform transmission line structures can be characterized in terms of a distributed series inductance and series resistance (for conductor loss) and a distributed shunt capacitance and shunt conductance (for dielectric loss).

To simplify the analysis of uniform transmission lines, the distributed inductance can be obtained directly from the distributed capacitance, as described in the following section.

2.1 Determination of Distributed Inductance for Uniform Transmission Lines

To determine the distributed inductance from the capacitance for a single two-conductor uniform transmission line embedded in a homogeneous dielectric

medium with permittivity ε and permeability μ_0, we consider the figure below [9].

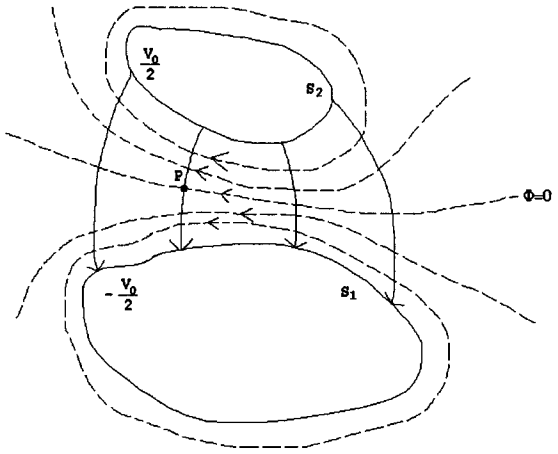

Figure 2.1 Two conductors in homogenous medium with electromagnetic and field lines.

All the flux lines from the line joining $\Phi = 0$ to $\Phi = V_0/2$ line link the current on S_2. If we choose path PS_2, which coincides with a line of electric force (and therefore is orthogonal to the flux lines), the flux linkage will be the total flux cutting this path. Therefore, since $|\mathbf{H}| = |\mathbf{E}|/\eta$ (for a TEM wave), where

$$\eta = \sqrt{\frac{\mu_0}{\varepsilon}} \tag{2.4}$$

is the intrinsic impedance of the medium, the flux cutting this path is

$$\Psi = \int_{P_1}^{S_2} \mu_0 H dl = \frac{\mu_0}{\eta} \int_{P_1}^{S_2} - \bar{E} \bullet d\bar{l} = \frac{\mu_0 V_0}{2\eta} . \tag{2.5}$$

The inductance of both conductors will be given by

$$L = 2\frac{\Psi}{I_0} = \frac{\mu_0 V_0}{\eta I_0} = \frac{\mu_0 Z_0}{\eta} = \frac{Z_0}{\sqrt{\mu_0 \varepsilon}} . \tag{2.6}$$

Using

$$C = \frac{\varepsilon \eta}{Z_0} , \tag{2.7}$$

it follows that

$$L = \frac{\mu_0 \varepsilon}{C} . \tag{2.8}$$

As was stated earlier, this equation is valid for a single homogenous medium. In order to calculate the distributed inductance for multi-layered dielectric media, all the dielectric media are removed and replaced with air. The distributed capacitance for the air-filled medium, C_{air}, is determined from the solution of the Laplace equation. The distributed inductance is calculated from (2.8) with $C = C_{air}$ and $\varepsilon = \varepsilon_0$. This means that two separate capacitance calculations have

to be made. The first is with all the dielectric media in place for determining C and the second is with all the dielectric media replaced with air to determine L from C_{air}.

2.2 Stripline and Microstrip

The quasi-static technique can be used at lower frequencies to determine the characteristics of uniform transmission lines, such as stripline and microstrip (see Figure 2.2 and Figure 2.3 Microstrip, respectively).

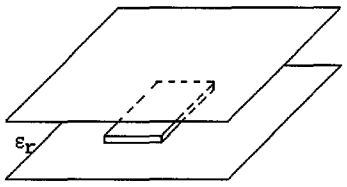

Figure 2.2 Stripline

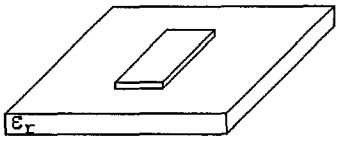

Figure 2.3 Microstrip

To illustrate the computation of the transmission line parameters by electromagnetic analysis, the simple stripline and microstrip structures will be solved by an approximate electrostatic analysis based on the method of separation of variables. The presentation given here is from [10].

2.3 Stripline

To simplify the analysis, the stripline structure is placed inside a sufficiently large conducting box of width a and height b, as shown in Figure 2.4.

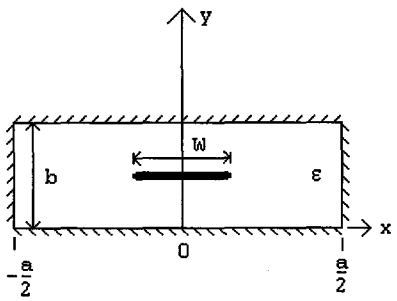

Figure 2.4 Stripline in large conducting box

We start with the Laplace equation:

$$\nabla^2\Phi = 0, \quad \text{for } |x| <= a/2, \quad 0 <= y <= b \qquad (2.9)$$

for the electric potential Φ, subject to the boundary conditions

$$\Phi(x,y) = 0, \qquad \text{at } x = +/- \ a/2, \tag{2.10a}$$

$$\Phi(x,y) = 0, \qquad \text{at } y = 0,b. \tag{2.10b}$$

Because of the slope discontinuity of Φ at y=b/2 (due to the surface charge density), $\bar{D}$ is also discontinuous at y = b/2. As a result, two solutions for $\Phi(x,y)$ must be found for the two regions $0 < y < b/2$ and $b/2 < y < b$. They are:

$$\Phi(x, y) = \begin{cases} \sum_{\substack{n=1 \\ \text{odd}}}^{\infty} A_n \cos\left(\frac{n\pi x}{a}\right) \sinh\left(\frac{n\pi y}{a}\right) \\ \qquad\qquad \text{for } 0 \le y \le b/2 \\ \sum_{\substack{n=1 \\ \text{odd}}}^{\infty} B_n \cos\left(\frac{n\pi x}{a}\right) \sinh\left(\frac{n\pi (b-y)}{a}\right) \\ \qquad\qquad \text{for } b/2 \le y \le b \end{cases} \tag{2.11}$$

Because the potential is continuous at y=b/2, $A_n = B_n$. Since

$$E_y = -\frac{\partial \Phi}{\partial y}, \tag{2.12}$$

the electric field in the two regions is given by

$$E_y = \begin{cases} -\sum_{\substack{n=1 \\ \text{odd}}}^{\infty} A_n \left(\frac{n\pi}{a}\right) \cos\left(\frac{n\pi x}{a}\right) \cosh\left(\frac{n\pi y}{a}\right) & \text{for } 0 \le y < b/2 \\ \sum_{\substack{n=1 \\ \text{odd}}}^{\infty} A_n \left(\frac{n\pi}{a}\right) \cos\left(\frac{n\pi x}{a}\right) \cosh\left(\frac{n\pi}{a}(b-y)\right) & \text{for } b/2 \le y < b \end{cases} \tag{2.13}$$

From the normal electric field at the surface of the conductor, the surface charge density at y = b/2 can be expressed as

$$\rho_s(x) = 2\varepsilon_0\varepsilon_r \sum_{\substack{n=1 \\ \text{odd}}}^{\infty} A_n \left(\frac{n\pi}{a}\right) \cos\left(\frac{n\pi x}{a}\right) \cosh\left(\frac{n\pi b}{2a}\right) . \tag{2.14}$$

If the surface charge density is assumed constant ($\rho_s = 1\ C/m^2$) on the surface of the strip and zero everywhere else, then solving for A_n gives

$$A_n = \frac{2a \sin\left(\frac{n\pi W}{2a}\right)}{(n\pi)^2 \varepsilon_0\varepsilon_r \cosh\left(\frac{n\pi b}{2a}\right)} . \tag{2.15}$$

The voltage of the center strip, relative to the ground plane is obtained by integrating the electric field as

$$V = -\int_0^{b/2} E_y(x = 0, y)dy = 2 \sum_{\substack{n=1 \\ \text{odd}}}^{\infty} A_n \sinh\left(\frac{n\pi b}{4a}\right) . \tag{2.16}$$

The total charge per unit length on the center strip is

$$Q = \int_{-W/2}^{W/2} \rho_s(x)dx = W . \qquad (2.17)$$

Dividing 2.17 by 2.16 gives the approximate distributed capacitance of the stripline structure as

$$C = \frac{Q}{V} = \frac{W}{\sum_{\substack{n=1 \\ \text{odd}}}^{\infty} \frac{2a \sin(\frac{n\pi W}{2a}) \sinh(\frac{n\pi b}{4a})}{(n\pi)^2 \varepsilon_0 \varepsilon_r \cosh(\frac{n\pi b}{2a})}} \quad (F/m) . \qquad (2.18)$$

2.4 Microstrip

For the case of microstrip, a similar analysis is given in [10] and is summarized below.

Once again, the analysis is simplified by placing the microstrip structure inside a sufficiently large conducting box of width a and infinite height, as shown in Figure 2.5.

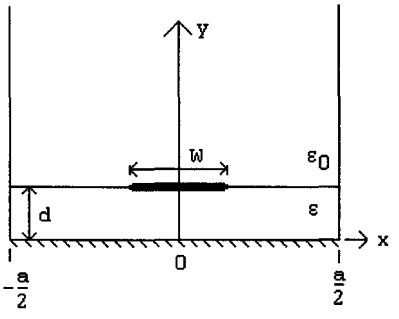

Figure 2.5 Microstrip in large conducting box.

We start again with the Laplace equation

$$\nabla^2\Phi = 0, \quad \text{for } |x| <= a/2, \quad 0 <= y <= \infty \tag{2.19}$$

and the boundary conditions

$$\Phi(x,y) = 0, \qquad \text{at } x = +/- a/2, \tag{2.20a}$$

$$\Phi(x,y) = 0, \qquad \text{at } y = 0,\infty. \tag{2.20b}$$

The slope of Φ is discontinuous at y=d due to the change in ε and the surface charge density on the conductors. As a result, two solutions for $\Phi(x,y)$ must be found for the two regions $0 < y < d$ and $d < y < \infty$. They are:

$$\Phi(x, y) = \begin{cases} \sum_{\substack{n=1 \\ \text{odd}}}^{\infty} A_n \cos\left(\frac{n\pi x}{a}\right) \sinh\left(\frac{n\pi y}{a}\right) & \text{for } 0 <= y <= d \\ \sum_{\substack{n=1 \\ \text{odd}}}^{\infty} B_n \cos\left(\frac{n\pi x}{a}\right) e^{-\frac{n\pi(y-d)}{a}} & \text{for } d <= y <= \infty \end{cases} . \tag{2.21}$$

Because the potential is continuous at y=d,

$$A_n \sinh\left(\frac{n\pi x}{a}\right) = B_n e^{-\frac{n\pi d}{a}} . \tag{2.22}$$

Since

$$E_y = -\frac{\partial \Phi}{\partial y}, \tag{2.23}$$

the electric field in the two regions is given by

$$E_y = \begin{cases} -\sum_{\substack{n=1 \\ \text{odd}}}^{\infty} A_n \left(\frac{n\pi}{a}\right) \cos\left(\frac{n\pi x}{a}\right) \cosh\left(\frac{n\pi y}{a}\right) & \text{for } 0 \le y < d \\ \sum_{\substack{n=1 \\ \text{odd}}}^{\infty} A_n \left(\frac{n\pi}{a}\right) \cos\left(\frac{n\pi x}{a}\right) \sinh\left(\frac{n\pi d}{a}\right) e^{-\frac{n\pi(y-d)}{a}} & \text{for } d \le y < \infty \end{cases} \tag{2.24}$$

The surface charge density at y = d is given by

$$\rho_s(x) = \varepsilon_0 \sum_{\substack{n=1 \\ \text{odd}}}^{\infty} A_n \left(\frac{n\pi}{a}\right) \cos\left(\frac{n\pi x}{a}\right) \left[\sinh\left(\frac{n\pi d}{a}\right) + \varepsilon_r \cosh\left(\frac{n\pi d}{a}\right)\right]. \tag{2.25}$$

If the surface charge density is assumed to be constant ($\rho_s = 1$ C/m^2) on the strip and zero everywhere else, then solving for A_n results in

$$A_n = \frac{4a \sin\left(\frac{n\pi W}{2a}\right)}{(n\pi)^2 \varepsilon_0 \left[\sinh\left(\frac{n\pi d}{a}\right) + \varepsilon_r \cosh\left(\frac{n\pi d}{a}\right)\right]}. \tag{2.26}$$

The voltage of the strip, relative to the bottom ground plane is

$$V = -\int_0^d E_y(x = 0, y)dy = \sum_{\substack{n = 1 \\ \text{odd}}}^{\infty} A_n \sinh\left(\frac{n\pi d}{a}\right) . \qquad (2.27)$$

The total charge per unit length on the center strip is given by

$$Q = \int_{-W/2}^{W/2} \rho_s(x)dx = W . \qquad (2.28)$$

Dividing (2.28) by (2.27) results in the approximate distributed capacitance of the microstrip and is given by

$$C = \frac{Q}{V} = \frac{W}{\sum_{\substack{n = 1 \\ \text{odd}}}^{\infty} \frac{4a \sin\left(\frac{n\pi W}{2a}\right) \sinh\left(\frac{n\pi d}{a}\right)}{(n\pi)^2 \varepsilon_0 \left[\sinh\left(\frac{n\pi d}{a}\right) + \varepsilon_r \cosh\left(\frac{n\pi d}{a}\right)\right]}} \quad (F/m) . \qquad (2.29)$$

These calculations are for the very simple case of a single conductor in a simple medium and are done for the two-dimensional case. The derivation for numerical solutions of general multiple strips in lossy multi-layered dielectric media becomes prohibitively complex. This complexity has led to the development of many other numerical techniques to determine the circuit parameters of more complex structures.

3. NETWORK ANALOG METHOD

The network analog method is an efficient technique for solving the finite difference approximation of the Laplace equation by transforming the quasi-electrostatic problem into a corresponding network problem. The analogous network is described by an impedance matrix relating nodal voltages and currents. From the impedance matrix, the capacitance matrix of multi-conductor structures in planar multilayered dielectric media can be determined. As was shown in Chapter 2, other relevant circuit parameters can also be determined from the capacitance matrix.

The network analog method is implemented by first discretizing the entire structure into a grid. Next, each discretized layer is represented as a series of network elements, with each element chosen appropriately. The choice for the network elements will be explained later. The impedance matrix is determined and then used to obtain the capacitance matrix for the structure. While there are simulators, such as SPICE, which can be used to sequentially determine the impedance matrix elements, these programs are slow and

cumbersome to use for this purpose, even for a small discretized area. In contrast, by taking advantage of the properties of the resulting network, an efficient approach for determining the impedance matrix is used in the network analog method.

The derivation of the equations necessary to determine the impedance matrix using the network analog method will follow the historical development of the method. First the work done by Lennartsson [6] for two-dimensional single layered structures is described. This is followed by Tripathi's extensions to two-dimensional [7] and three-dimensional [8] multi-conductor structures in general multilayered lossy dielectric media.

3.1 Analysis of Two-dimensional Single Layered Structures

Starting with a discretized, single layered structure such as that shown in Figure 3.1, we wish to calculate the impedance matrix [Z]. To do this, each column is electrically isolated, resulting in Figure 3.2. This is known as the diagonalized domain.

Calculating the impedance at any node in the diagonalized domain is very quick and accurate.

Once the impedance at all nodes of interest has been calculated in the diagonalized domain, the diagonalized matrix is transformed back into the impedance matrix, from which the desired parameters can be determined, as was shown in Chapter 2.

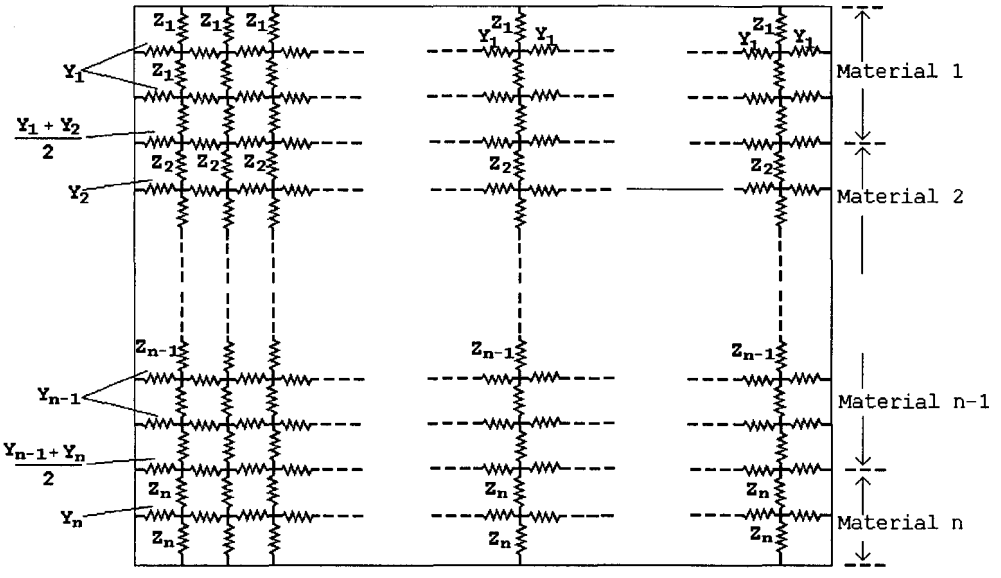

Figure 3.1 Network Analog for discretized material

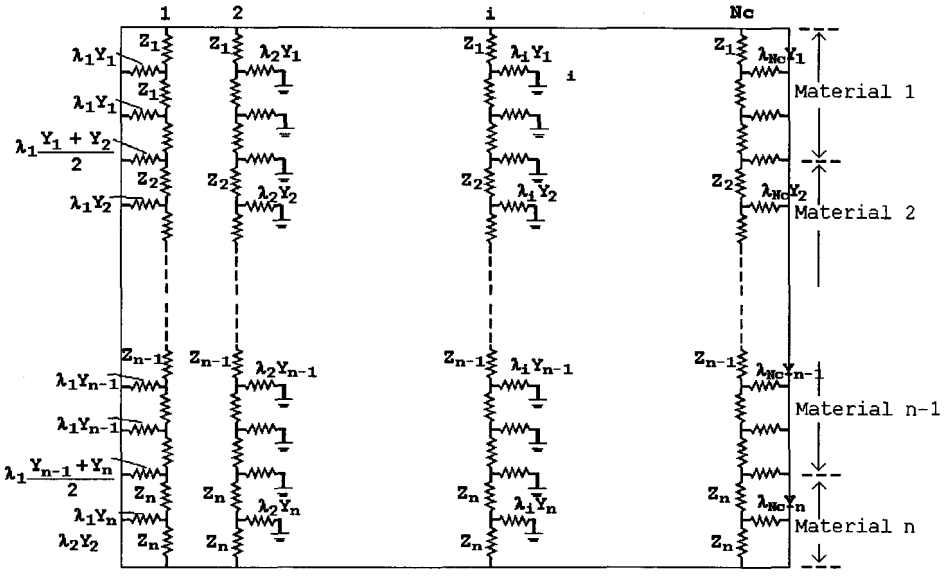

Figure 3.2 Electrically isolated network

Lennartsson[6] showed that the impedance matrix at any level L can be calculated using the recurrence relationship

$$Z_L = [Z_{L-1}^{-1} + g_{L-1}P]^{-1} + z_L U \tag{3.1}$$

where

$$Z_1 = z_1 U \tag{3.2}$$

and

$$P = \begin{vmatrix} 2 & -1 & 0 & - & - & - & 0 \\ -1 & 2 & -1 & 0 & - & - & 0 \\ 0 & -1 & 2 & -1 & 0 & - & 0 \\ \bullet & \bullet & \bullet & \bullet & \bullet & \bullet & \bullet \\ \bullet & \bullet & \bullet & \bullet & \bullet & \bullet & \bullet \\ 0 & - & - & - & -1 & 2 & -1 \\ 0 & - & - & - & - & -1 & 2 \end{vmatrix}. \tag{3.3}$$

As equation (3.1) is a recurrence equation, it is well suited for computer work. However it is very slow and cumbersome to use because it involves two matrix inversions.

Lennartsson noted that because P is symmetric, there is an orthogonal matrix A such that

$$[A]^T[P][A] = \begin{bmatrix} \lambda_1 & & & & \\ & \lambda_2 & & & \\ & & \lambda_3 & & \\ & & & \ddots & \\ & & & & \lambda_n \end{bmatrix} \tag{3.4}$$

with

$$[A]^T[A] = U. \tag{3.5}$$

λ_i are the eigenvalues of P.

In (3.4) the expressions for λ_i and [A] are known and given by

$$\lambda_i = 4\sin^2\left[\frac{i\pi}{2(N_c + 1)}\right], \quad i = 1, N_c \tag{3.6}$$

and

$$\{a_{ij}\} = \sqrt{\frac{2}{(N_c + 1)}}\sin\left(\frac{ij\pi}{N_c + 1}\right), \quad i = 1, N_c, \quad j = 1, N_c. \tag{3.7}$$

Using (3.1) and [A], Lennartsson showed that

$$[\hat{Z}] = [A][Z][A]. \tag{3.8}$$

The matrix on the left side of (3.8) represents the diagonalized impedance matrix. As this matrix is diagonal,

$$\hat{Z}_{ij} = 0 \text{ for } i \neq j.$$

Because A is involutary ($[A] = [A]^T = [A]^{-1}$),

$$[Z] = [A][\hat{Z}][A]. \tag{3.9}$$

It therefore becomes a simple matter to determine the impedance matrix once the diagonalized matrix has been found.

By examining Figure 3.2, we can see that the impedance is equal to:

$$\hat{Z}_j^L = \frac{1}{\frac{1}{(\alpha_u^L)_j} + \frac{1}{(\alpha_l^L)_j} + \lambda_j y^L}, \quad j = 1 \ldots N_c \text{ at level L.} \tag{3.10}$$

This is simply the parallel combination of the Thevenin resistance looking up, the Thevenin resistance looking down and the equivalent conductance to ground. The Thevenin resistance from any node, up or down, at any level L is given by:

$$\alpha_{u,l}^{L+1} = \frac{1}{\frac{1}{(\alpha_{u,L}^L)} + \lambda_j y^L} + z^{L+1} \tag{3.11}$$

where

$$\alpha^{L}_{u,l} = z^{L}_{u,l} . \tag{3.12}$$

As Lennartsson pointed out, a suitable choice for the network elements is given by:

$$z^{L} = \varepsilon_{r} \tag{3.13a}$$

and

$$z^{L} = (\varepsilon_{r1} + \varepsilon_{r2})/2 \tag{3.13b}$$

at the interface for the elements joining two surfaces. The reason for this choice will be given later.

3.2 Analysis of Two-dimensional Multi-layered Structures

Tripathi and Bucolo[7] expanded on this approach to include thick and multilevel conductors. This was accomplished by including the transfer impedances ($\hat{Z}_{km}$). The equation in the diagonal domain is as follows:

$$\hat{Z}_{km} = \frac{1}{\frac{1}{(\alpha^{k}_{u})_{j}} + \lambda_{j} y^{k}} \bullet \frac{\frac{1}{(\alpha^{m}_{u})_{j}}}{\frac{1}{(\alpha^{m}_{u})_{j}} + \frac{1}{(\alpha^{m}_{l})_{j}} + \lambda_{j} y^{m}} \bullet \prod_{q=m+\mathrm{sgn}(k-m)}^{q=k-\mathrm{sgn}(k-m)} \frac{\frac{1}{(\alpha^{q}_{u})_{j}}}{\frac{1}{(\alpha^{q}_{u})_{j}} + \lambda_{j} y^{q}} . \tag{3.14}$$

As they noted, this equation represents the fraction of current on the level m node which reaches the level k node, multiplied by the impedance to the

upper ground at level k, including the admittance $\lambda_j y^k$. Due to symmetry for a passive network, $\hat{Z}_{km} = \hat{Z}_{mk}$. The total impedance network, then, is as follows:

$$\begin{bmatrix} V_1 \\ \vdots \\ V_P \end{bmatrix} = \begin{bmatrix} [z]_{11} & \cdots & [z]_{1P} \\ \vdots & \ddots & \vdots \\ [z]_{P1} & \cdots & [z]_{PP} \end{bmatrix} \begin{bmatrix} I_1 \\ \vdots \\ I_P \end{bmatrix} \tag{3.15}$$

3.3 Analysis of Three-dimensional Multi-layered Structures

Tripathi and Bucolo extended this technique further when they derived the equations necessary to analyze three dimensional multi-conductor, lossy, layered structures[8].

The biggest difference in the three-dimensional technique is the change of the tridiagonal matrix, P, (3.3), to a block-tridiagonal matrix.

The eigenvalues of this new matrix are given by:

$$\lambda_{i,j} = 4 - 2\left[\cos\left[\frac{i\pi}{(N_r + 1)}\right] + \cos\left[\frac{j\pi}{N_c + 1}\right]\right], \quad i=1,N_r;\ j=1,N_c. \tag{3.16}$$

There are N_c nodes in the 'x' direction and N_r nodes in the 'y' direction at each of the levels in the 'z' direction. The [A] matrix now contains $(N_c x N_r) x (N_c x N_r)$ elements which are given by:

$$\{a_{m,n}\} = \frac{2}{\sqrt{(N_c + 1)\,(N_r + 1)}} \sin\left[\frac{(ixm)\pi}{(N_r + 1)}\right] \sin\left[\frac{(jxn)\pi}{(N_c + 1)}\right] \quad (3.17)$$

$i=1,2,\ldots,N_r;\ m=1,2,\ldots,N_r$

$j=1,2,\ldots,N_c;\ n=1,2,\ldots,N_c$

At any level L, the diagonalized input impedance matrix is given by:

$$[\hat{Z}_{L,L}]_{i,j} = \frac{1}{\frac{1}{(\alpha_u^L)_{i,j}} + \frac{1}{(\alpha_l^L)_{i,j}} + \lambda_{i,j}\frac{y^{L-1} + y^{L+1}}{2}} \quad (3.18)$$

where

$$\alpha_{u,l}^{k+1})_{i,j} = \frac{1}{\frac{1}{(\alpha_{u,l}^k)_{i,j}} + \lambda_{i,j}\frac{y^k + y^{k+1}}{2}} + z^{k+1} \quad (3.19)$$

The diagonalized transfer impedance matrix for the three dimensional case is given by

$$\left[\hat{Z}_{km}\right]_{i,j} = \frac{1}{\frac{1}{(\alpha_u^k)_{i,j}} + \lambda_{i,j}y^k} \bullet \frac{\frac{1}{(\alpha_u^m)_{i,j}}}{\frac{1}{(\alpha_u^m)_{i,j}} + \frac{1}{(\alpha_l^m)_{i,j}} + \lambda_{i,j}y^m} \bullet \prod_{q=m+\mathrm{sgn}(k-m)}^{q=k-\mathrm{sgn}(k-m)} \frac{\frac{1}{(\alpha_u^q)_{i,j}}}{\frac{1}{(\alpha_u^q)_{i,j}} + \lambda_{i,j}y^q} \quad . \quad (3.20)$$

Note that this equation is identical to (3.14) and that (3.18) is identical to (3.10), except for the added column notation (j subscript). The difference between the three-dimensional and the two-dimensional methods lies in the calculation of the [λ], [α], and [A] matrices.

3.4 Calculation of Capacitance matrix

As was stated earlier, the proper choice for the network elements is the relative permittivity of the material, or in the case of a transition layer, the average relative permittivity of the two adjacent layers. The reason for this choice was given by Lennartsson[6].

Any network can be characterized by its impedance matrix as follows:

$$[V] = [Z][I], \tag{3.21}$$

where [V] represents the voltage at all the nodes, [Z] represents the impedance matrix, and [I] represents the input current at the nodes.

If [V] and [Z] are known, [I] is determined by inverting [Z] and multiplying by [V]:

$$[I] = [Y][V], \tag{3.22}$$

where [Y] is the inverse of [Z] and is the admittance matrix.

Writing this in a different form and assuming a constant voltage at each node of a given conductor, we express the relationship between [I] and [V] as

$$I_1 = y_{11}V_1 + y_{12}V_2 + \ldots + y_{1(n-1)}V_{n-1} + y_{1n}V_n$$

$$I_2 = y_{21}V_1 + y_{22}V_2 + \ldots + y_{2(n-1)}V_{n-1} + y_{2n}V_n$$

.

.

.

$$I_n = y_{n1}V_1 + y_{n2}V_2 + \ldots + y_{n(n-1)}V_{n-1} + y_{nn}V_n \tag{3.23}$$

where I_n is the total input current on conductor n and V_n is the voltage on conductor n. Note that in this form, I_n is not the current at node n and V_n is not the voltage at node n.

In this form, y_{nn} represents the sum of the elements in the admittance matrix for the conductor n and y_{mn} is the sum of the transfer elements in the admittance matrix for the two conductors m and n. Since the admittance matrix is symmetric, $y_{mn} = y_{nm}$.

Moving back into field theory, the relationship between the charges on the conductors (per unit length

for two-dimensional systems) and the voltages on the strips is given by

$$Q_1 = c_{11}V_1 + c_{12}V_2 + \ldots + c_{1n}V_n$$

$$Q_2 = c_{21}V_1 + c_{22}V_2 + \ldots + c_{2n}V_n$$

.

.

.

$$Q_n = c_{n1}V_1 + c_{n2}V_2 + \ldots + c_{nn}V_n \qquad (3.24)$$

Lennartsson then showed that because of (3.24) and (3.23) and the choice of the network elements, $c_{nn} = \varepsilon_0 y_{nn}$.

This gives the capacitance matrix, which is the key to determining other characteristic parameters of these structures.

As Tripathi and Bucolo[7] showed, determination of the transmission line parameters is easily done once the admittance matrix has been found. For the case of single strips of width W and thickness T, the strip is discretized into N sections and the current at each node is solved under the assumption that the input voltage at each node is 1v at frequency ω rad/s. The distributed transmission line parameters then become:

$$C = \mathrm{Im}\left[\sum_{1}^{N} I_{node}\right] \Big/ \omega, \quad F/m \tag{3.26}$$

$$G = \mathrm{Re}\left[\sum_{1}^{N} I_{node}\right], \quad \Omega/m \tag{3.27}$$

and

$$L = \omega\mu_0\varepsilon_0 \Big/ \sum_{1}^{N} \mathrm{Im}\left[I_{node}\right], \quad H/m \text{ with all dielectric layers removed.} \tag{3.28}$$

For the case of multiple strips, the summations above are done over the number of transfer nodes. For example, in the case of two conductors, the first one is discretized into N sections and the second is discretized into M sections. The summation is carried out for the nodes I_{NM}.

It is clear to see that the summations are not done for each parameter, but, rather, once the [Y] matrix is obtained, the others can be easily obtained by simply dividing or multiplying by the proper constants.

3.5 Programming Considerations

The calculation of the 4 major matrices involved, namely the [A], [λ], [$\hat{Z}$] and the [α] matrices, is straightforward and well suited to computer work.

As was stated at the outset, however, the goal is to calculate the [Z] matrix for whatever structure we are analyzing. In order to accomplish this, two matrix multiplications will have to occur (e.g. [A][$\hat{Z}$][A]). Matrix multiplication is well suited for computer work, but given the relatively large size of [A], this can prove to be a very CPU intensive task. Using the fact that [$\hat{Z}$] is a diagonal matrix, a better technique (equation) can be derived for the calculation of the [Z] matrix.

The equation for the [Z] matrix is given here:

$$\left[Z\right]_{i,j} = \sum_{k=1}^{N_c x N_r} A_{i,k}\hat{Z}_{k,k}A_{k,j} \qquad (3.25)$$

Note that the elements of [A] are of the form $\Gamma\sin(a)\sin(b)$.

Therefore, $A_{i,k}*A_{k,j}$ will be of the form $\Gamma^2\sin(a)\sin(b)\sin(c)\sin(d)$. Since Γ is independent of k,

it can be taken outside the summation. The rest of the equation can be rearranged as

$$\frac{1}{4} * (\cos(a-b) - \cos(a+b)) * (\cos(c-d) - \cos(c+d))$$

This rearrangement can save significant processing time and is used in the code.

4. APPLICATION

The validation of this technique was done for both the two- and three-dimensional cases. In order to check the accuracy of the implemented code, and to set benchmarks for its performance, it was compared to the performance of the code generated from the technique presented by Tripathi and Bucolo[7] for two-dimensional structures. The code generated from [7] has been in use for many years, and its validity and accuracy have been demonstrated.

4.1 Two-dimensional Analysis

For the two-dimensional case, the results in several different configurations from both this implementation and that from Tripathi and Bucolo[7] (referred to as ML2DN) are compared.

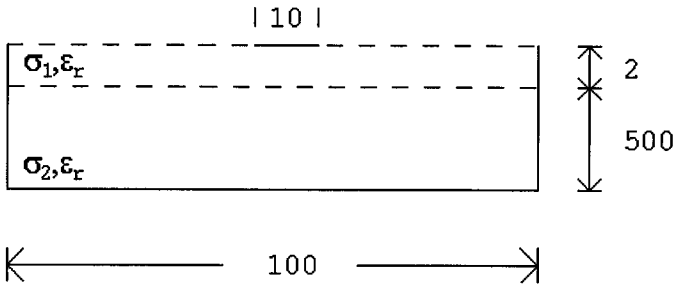

Figure 4.1 Two-dimensional, single conductor

a) $\sigma_1 = \sigma_2 = 0$; $\varepsilon_{r1} = \varepsilon_{r2} = 1$

	Present Technique	ML2DN
YD(1,1)(S/m)	(0.0,0.106753)	(0.0,0.106759)
YD(1,2)(S/m)	-------	-------
YD(2,2)(S/m)	-------	-------
CPU time(ms)	703	472

b) $\sigma_1 = \sigma_2 = 0$; $\varepsilon_{r1} = 3.9$ $\varepsilon_{r2} = 11.7$

	Present Technique	ML2DN
YD(1,1)(S/m)	(0.0,0.501499)	(0.0,0.501519)
YD(1,2)(S/m)	-------	-------
YD(2,2)(S/m)	-------	-------
CPU time(ms)	644	475

c) $\sigma_1 = 0$ $\sigma_2 = 10$ S/m; $\varepsilon_{r1} = 3.9$ $\varepsilon_{r2} = 11.7$

	Present Technique	ML2DN
YD(1,1)(S/m)	(3.809e-2,0.50320)	(3.809e-2,0.50322)
YD(1,2)(S/m)	-------	-------
YD(2,2)(S/m)	-------	-------
CPU time(ms)	644	475

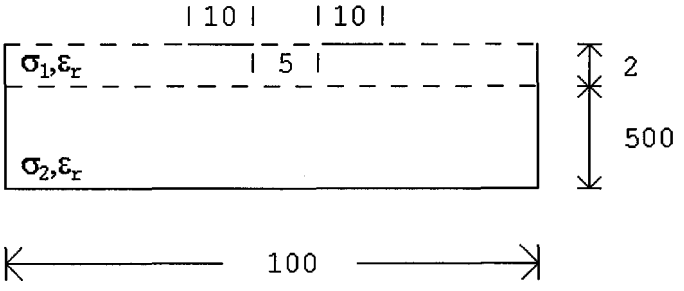

Figure 4.2 Two-dimensional, two conductors on the same level

a) $\sigma_1 = \sigma_2 = 0$; $\varepsilon_{r1} = \varepsilon_{r2} = 1$

	Present Technique	ML2DN
YD(1,1)(S/m)	(0.0,0.154865)	(0.0,0.154868)
YD(1,2)(S/m)	(0.0,-8.27146e-2)	(0.0,-8.27129e-2)
YD(2,2)(S/m)	(0.0,.154603)	(0.0,.154606)
CPU time(ms)	813	621

b) $\sigma_1 = \sigma_2 = 0$; $\varepsilon_{r1} = 3.9$, $\varepsilon_{r2} = 11.7$

	Present Technique	ML2DN
YD(1,1)(S/m)	(0.0,0.608854)	(0.0,.608866)
YD(1,2)(S/m)	(0.0,-.24403)	(0.0,-.244025)
YD(2,2)(S/m)	(0.0,.608034)	(0.0,.608046)
CPU time(ms)	790	630

c) $\sigma_1 = 0$, $\sigma_2 = 10$ S/m; $\varepsilon_{r1} = 3.9$, $\varepsilon_{r2} = 11.7$

	Present Technique	ML2DN
YD(1,1)(S/m)	(3.4322e-2,0.6106)	(3.4323e-2,0.61065)
YD(1,2)(S/m)	(-2.387e-3,-2.447)	(-2.386e-2,-2.447)
YD(2,2)(S/m)	(3.4311e-2,0.6098)	(3.4312e-2,0.6098)
CPU time(ms)	799	623

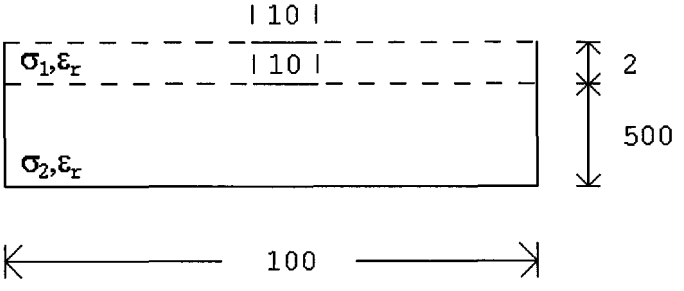

Figure 4.3 Two-dimensional, two conductors, different levels.

a) $\sigma_1 = \sigma_2 = 0$; $\varepsilon_{r1} = \varepsilon_{r2} = 1$

	Present Technique	ML2DN
YD(1,1)(S/m)	(0.0,0.414579)	(0.0,0.414582)
YD(1,2)(S/m)	(0.0,-0.35497)	(0.0,-0.35497)
YD(2,2)(S/m)	(0.0,0.414579)	(0.0,0.414582)
CPU time(ms)	862	669

b) $\sigma_1 = \sigma_2 = 0$; $\varepsilon_{r1} = 3.9$, $\varepsilon_{r2} = 11.7$

	Present Technique	ML2DN
YD(1,1)(S/m)	(0.0,1.4406)	(0.0,1.4406)
YD(1,2)(S/m)	(0.0,-1.3499)	(0.0,-1.3499)
YD(2,2)(S/m)	(0.0,1.9946)	(0.0,1.9947)
CPU time(ms)	861	680

c) $\sigma_1 = 0$, $\sigma_2 = 10$ S/m; $\varepsilon_{r1} = 3.9$, $\varepsilon_{r2} = 11.7$

	Present Technique	ML2DN
YD(1,1)(S/m)	(2.903e-3,1.441)	(2.903e-3,1.441)
YD(1,2)(S/m)	(-2.071e-3,-1.3501)	(-2.071e-3,-1.3501)
YD(2,2)(S/m)	(8.9061e-2,1.9948)	(8.9065e-2,1.9948)
CPU time(ms)	867	672

As the results from these two comparisons show, this technique is very accurate and fast for most applications. The difference between the two implementations is essentially 0. However, the processing time for the present technique is about 25% - 50% higher. Although not significant for small structures such as these, this processing time discrepancy can become significant as the number of discretized points becomes large.

4.2 Three-dimensional Analysis

To test the accuracy of the results for three-dimensional planar structures, this technique was compared to the results of those of Bhat and Koul[11]. The comparison was carried out over 7 different structures varying in layout and location and size of the pad.

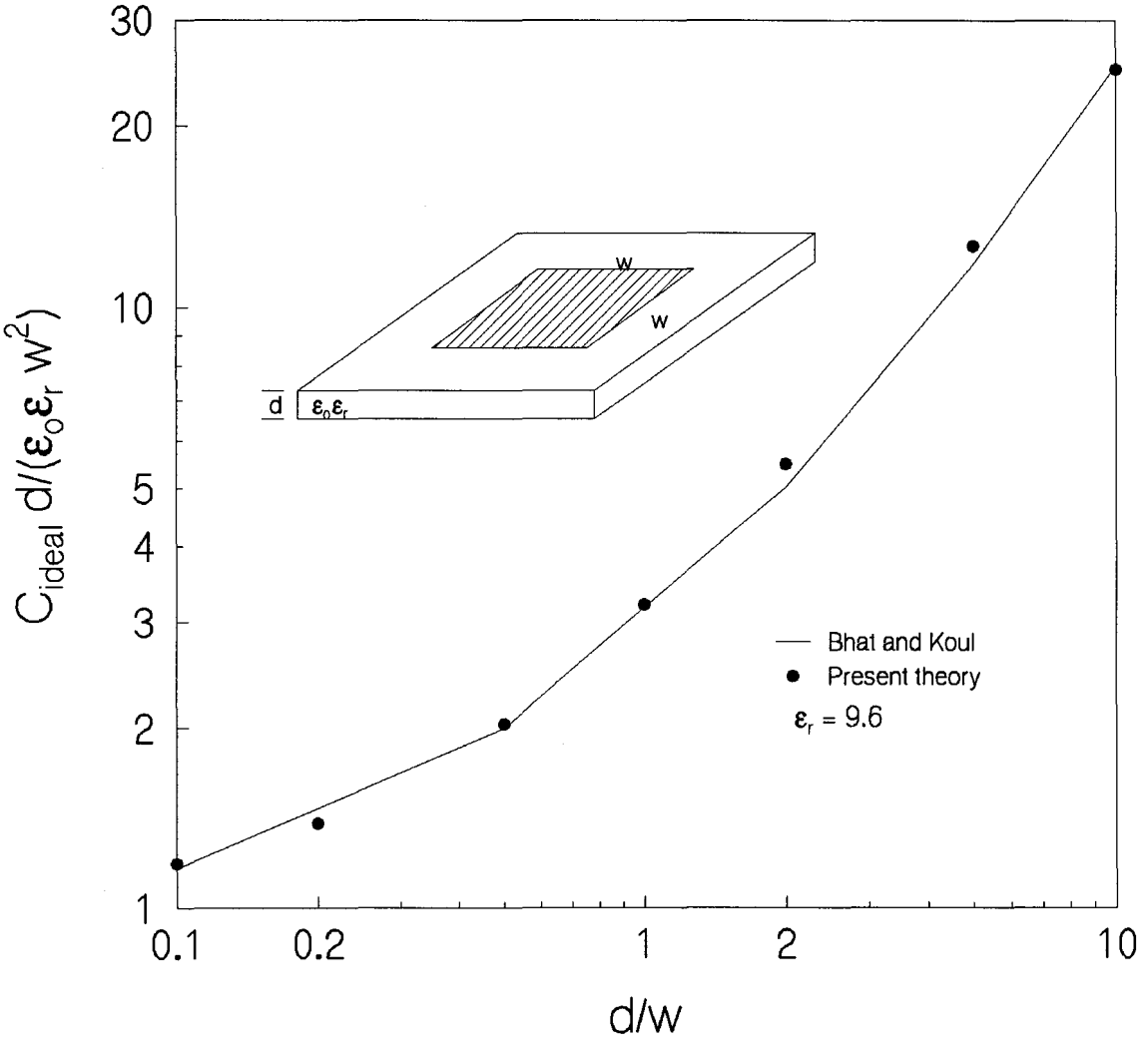

Figure 4.4 Comparison of normalized capacitance of microstrip square patch with Bhat and Koul[11]

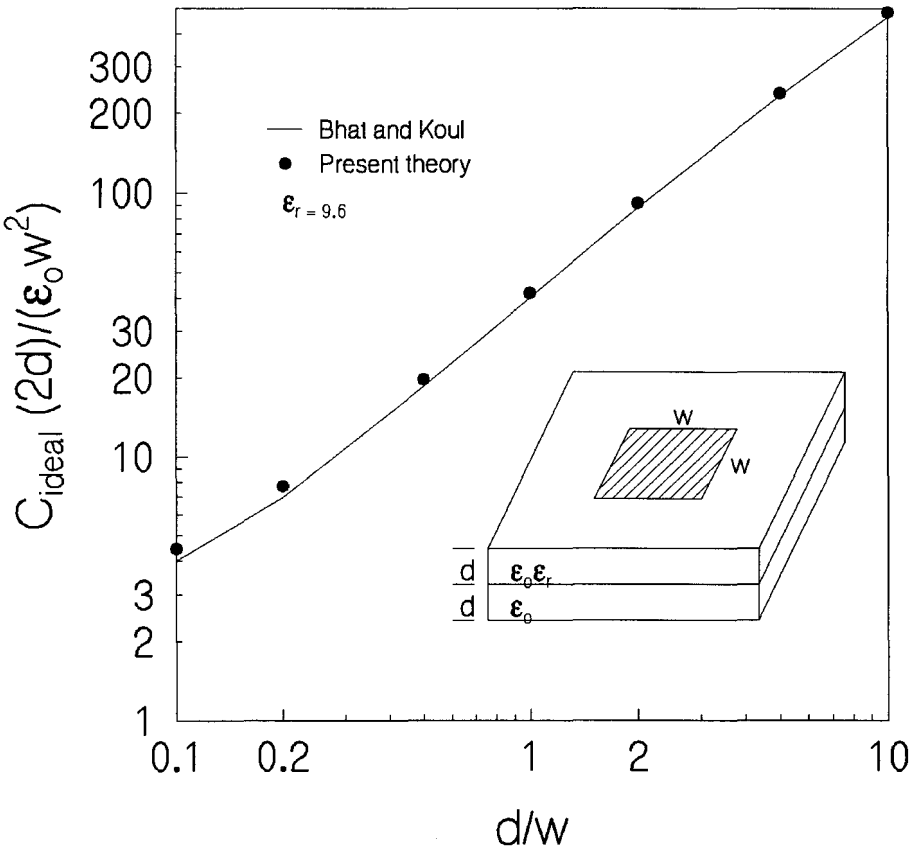

Figure 4.5 Comparison of normalized capacitance for square microstrip patch over two level dielectric material with Bhat and Koul[11].

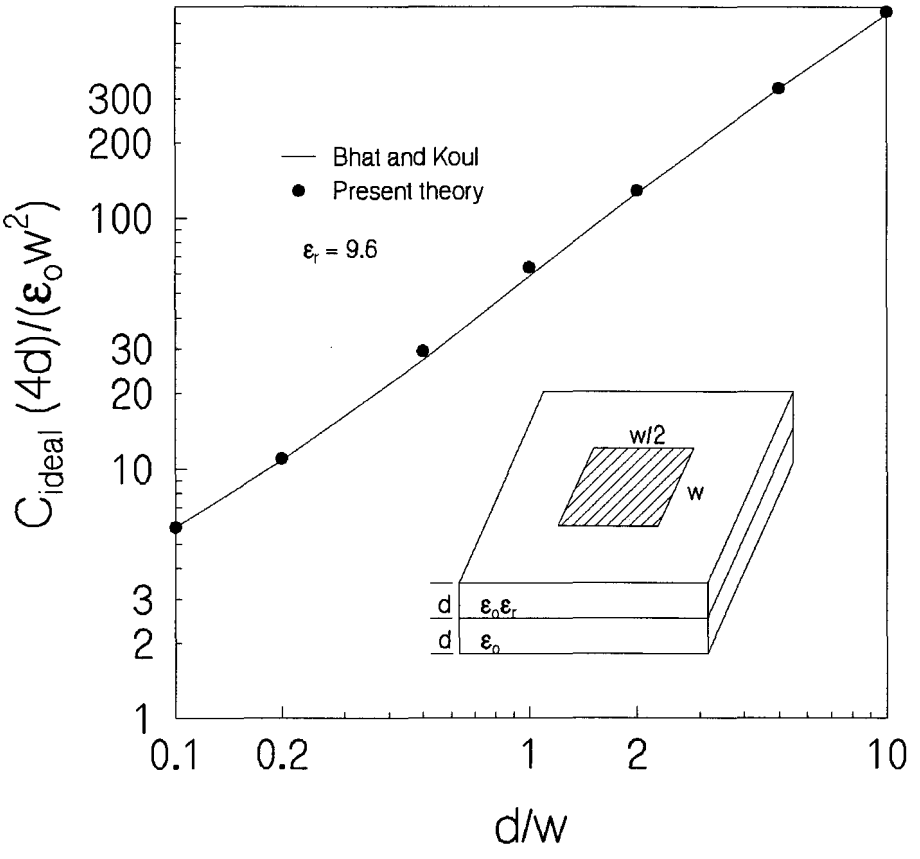

Figure 4.6 Comparison of normalized capacitance for rectangular microstrip patch over two level dielectric material with Bhat and Koul[11].

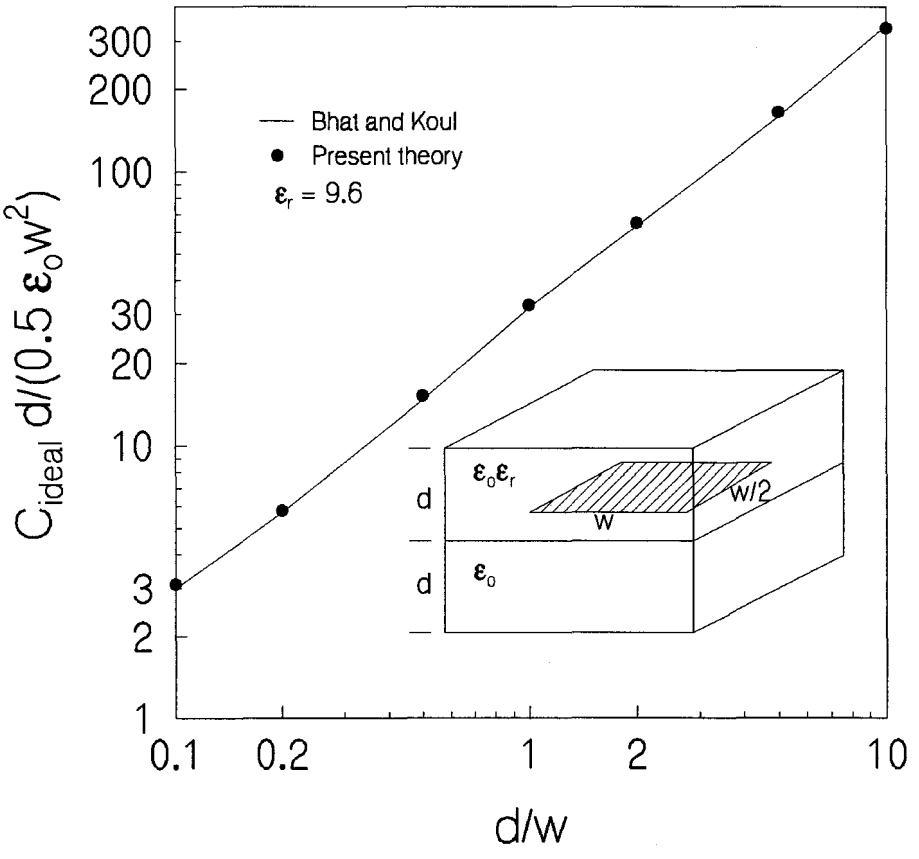

Figure 4.7 Comparison of of normalized capacitance of rectangular microstrip patch within a two level dielectric material with Bhat and Koul[11].

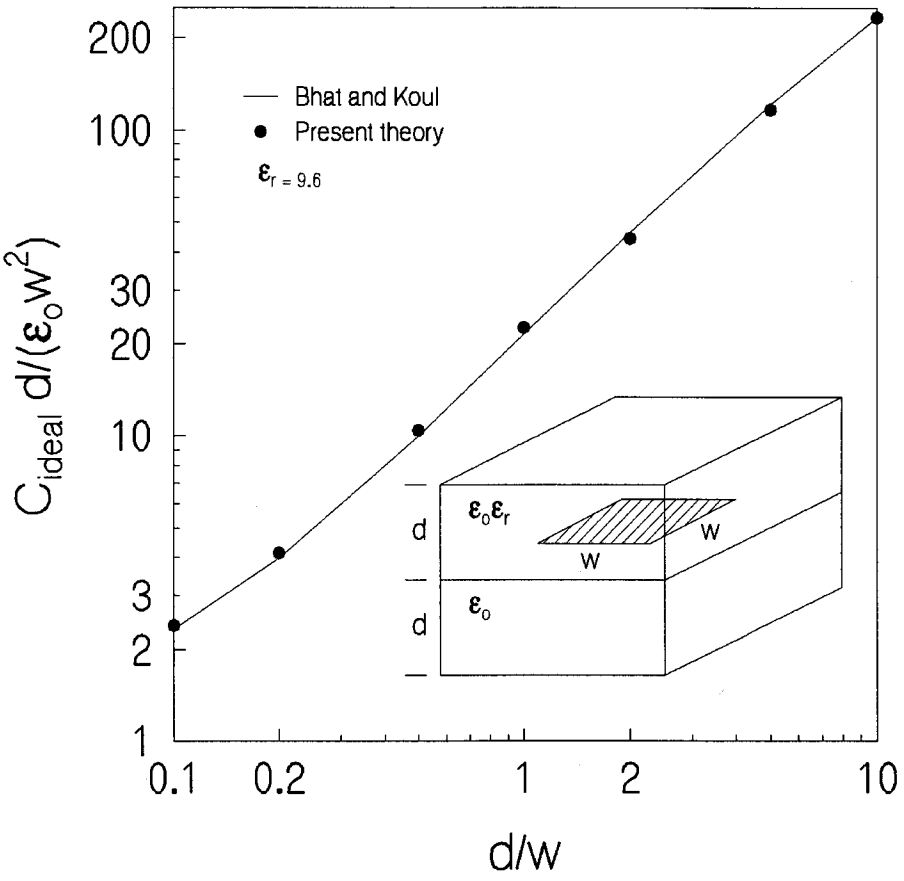

Figure 4.8 Comparison of normalized capacitance for square micropstrip patch within a two layered dielectric material with Bhat and Koul[11].

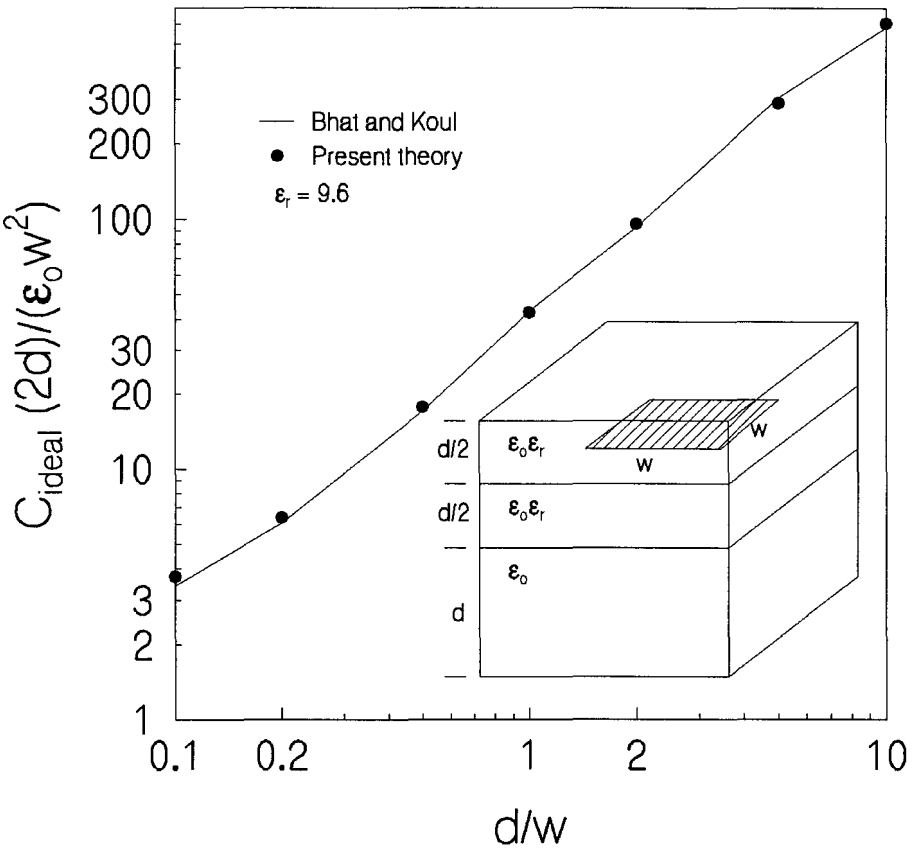

Figure 4.9 Comparison of normalized capacitance of square microstrip patch within three layer dielectric material with Bhat and Koul[11].

As one can clearly see from these graphs, the values calculated by this technique are in very good agreement with those obtained by Bhat and Koul[11].

Overall, the difference between the two techniques was less than 3.5% with most of the differences being less than 2%. The differences in values can be attributed primarily to the level of discretization used when carrying out these calculations. When the number of nodes was increased, the difference was generally below 1%.

While the above two analyses show the high accuracy of this technique, they do not say much about the speed of this technique. In the first analysis (the one with ML2DN), the program speed could be measured directly. However, in the second analysis, this was not possible. The processing time was measured, however, and in all cases the results were obtained in less than 5 minutes of processing time. (Note: These simulations were run on an HP969 series 3000).

In general the area of the pads was discretized to approximately 100 nodes (10x10) and the substrate width and length set to approximately 80 nodes. This implies 640 nodes per substrate layer. This is obviously a rather small discretization, which leads to the major drawback of this technique; namely, the cost of more accurate results is exponentially increased CPU time.

If the substrate is discretized to $N_c x N_r$, then just transforming the diagonalized Z matrix back into the regular Z matrix would take $N_c x N_r$ additions each with 3 multiplications (refer to equation 3.21). Increasing the number of nodes per layer would increase the number of additions (again, each with 3 multiplications) by that same factor. Therefore, increasing the number of nodes at each level by a factor of two would have a net effect of increasing the number of mathematical operations by at least six. In addition to this increase, the resolution of the dielectric layers would also have to increase, to keep the ratio of the width, length and depth constant.

One of the benchmarks for any analytical technique of this type must include its versatility. Any technique that is not easily applicable to many configurations is simply not as useful as a similar technique which accomplishes the same accuracy and speed but which also is versatile. This technique happens to be extremely well adapted to analyzing many different configurations and layouts, especially in the area of substrate profiles.

For example, having 5 different layers, each with a different permittivity and conductivity is not an issue in this technique. These types of configuration are just as easily analyzed as one in which the pad sits on a simple, single profile substrate.

One of the drawbacks to the way this technique is presently implemented, however, is that the pads must be in the form of a rectangle. Other configurations are not presently supported.

4.3 Three-dimensional Multi-conductor Analysis

As a final demonstration of this technique, two layouts were analyzed and the changes in coupling capacitance and coupling conductance were plotted as a function of the pad separation.

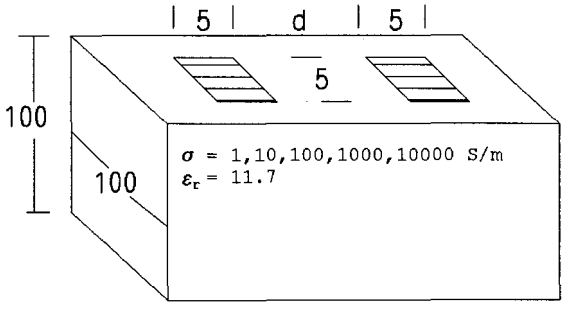

Figure 4.10 Three dimensional, two conductor, single-layered patch structure.

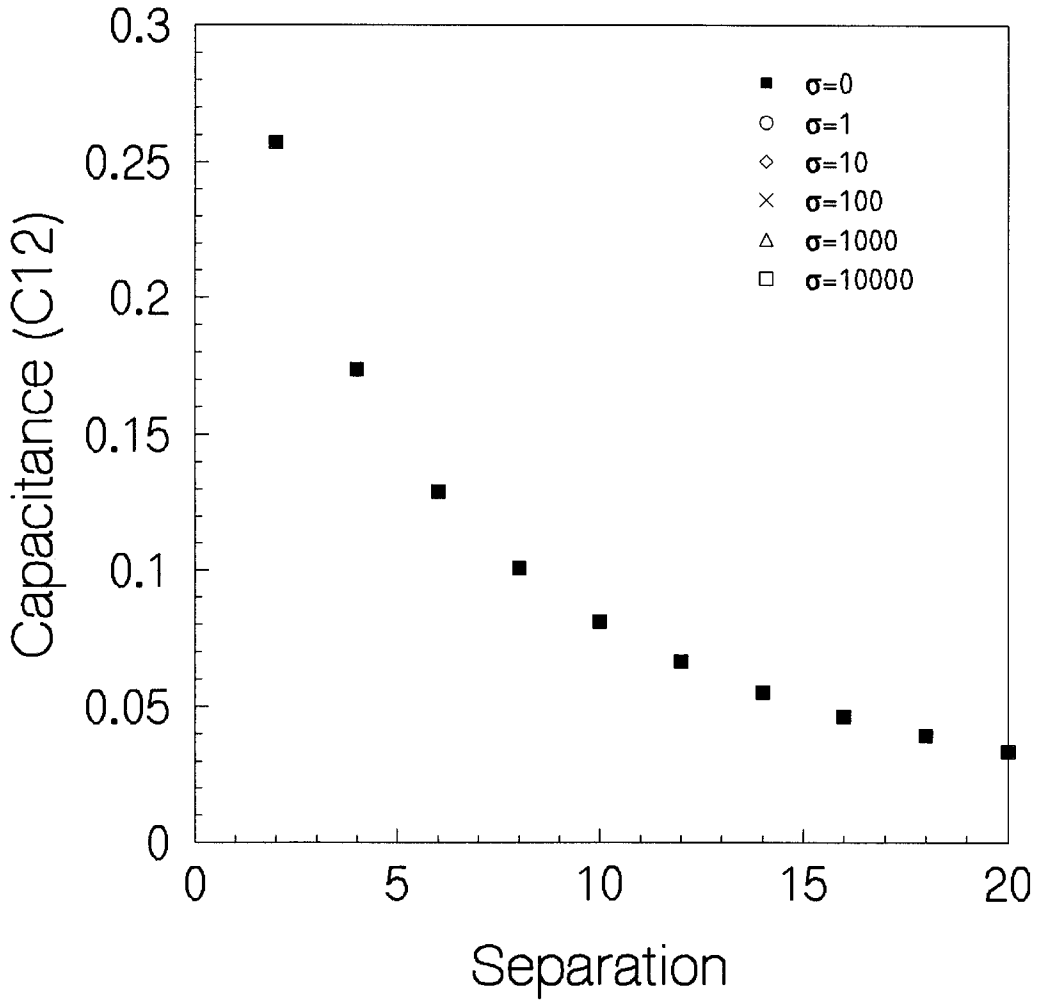

Figure 4.11 Coupling Capacitance vs. Separation for varying values of dielectric conductance.

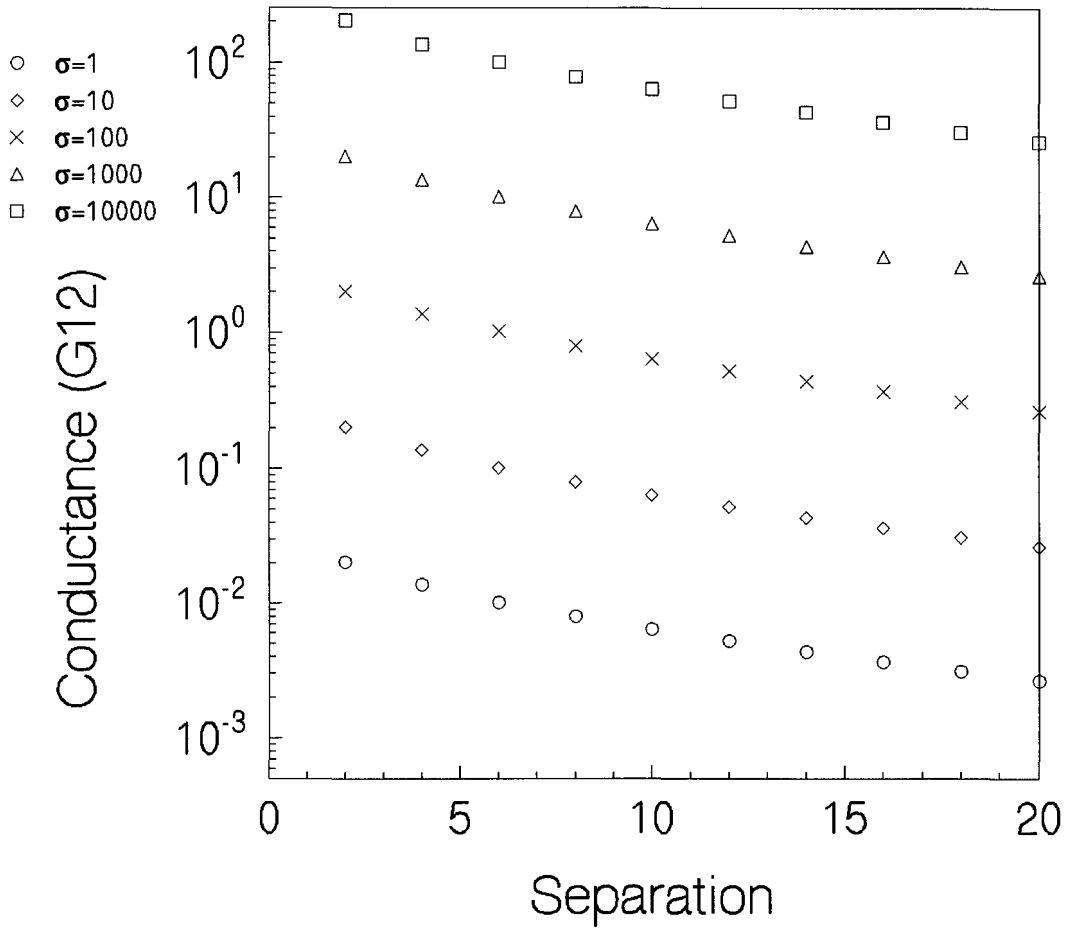

Figure 4.12 Coupling Conductance vs. Separation Distance for varying values of dielectric conductance.

In the first graph, Figure 4.11, the coupling capacitance was plotted as a function of the distance d between the right edge of the left patch and the left edge of the right patch. This was done for six different values of conductance of the dielectric

material (σ = 0, 1, 10, 100, 1000, 10000 S/m). As expected, the coupling capacitance is greatest when the two patches are closest together. Also, the change in the coupling capacitance as the conductance is changed is negligible (< 1%), which is why there appears to be only one set of data points.

The conductance was also calculated and plotted over the same range of values and these results are shown in Figure 4.12. As is shown, the coupling conductance does vary with separation. However, the coupling conductance is much more sensitive to the change in the dielectric conductance, as expected. Specifically, the change in coupling conductance is on the same order of magnitude as the dielectric media conductance change.

A second three-dimensional, two conductor analysis was performed in which the two conductors were at different levels, shown in Figure 4.13. In this analysis the separation distance, d, was measured as the distance between the left edge of each conductor as projected in an XY plane. In other words, the distance is measured based the projection of the second conductor into the top plane.

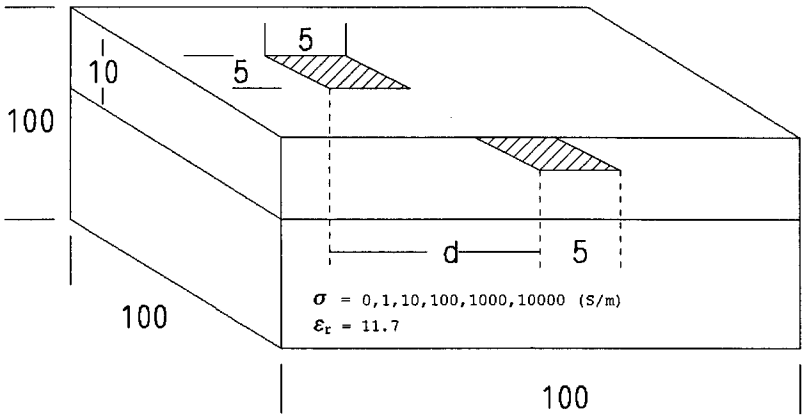

Figure 4.13 Three dimensional, two conductor, multi-layered patch structure.

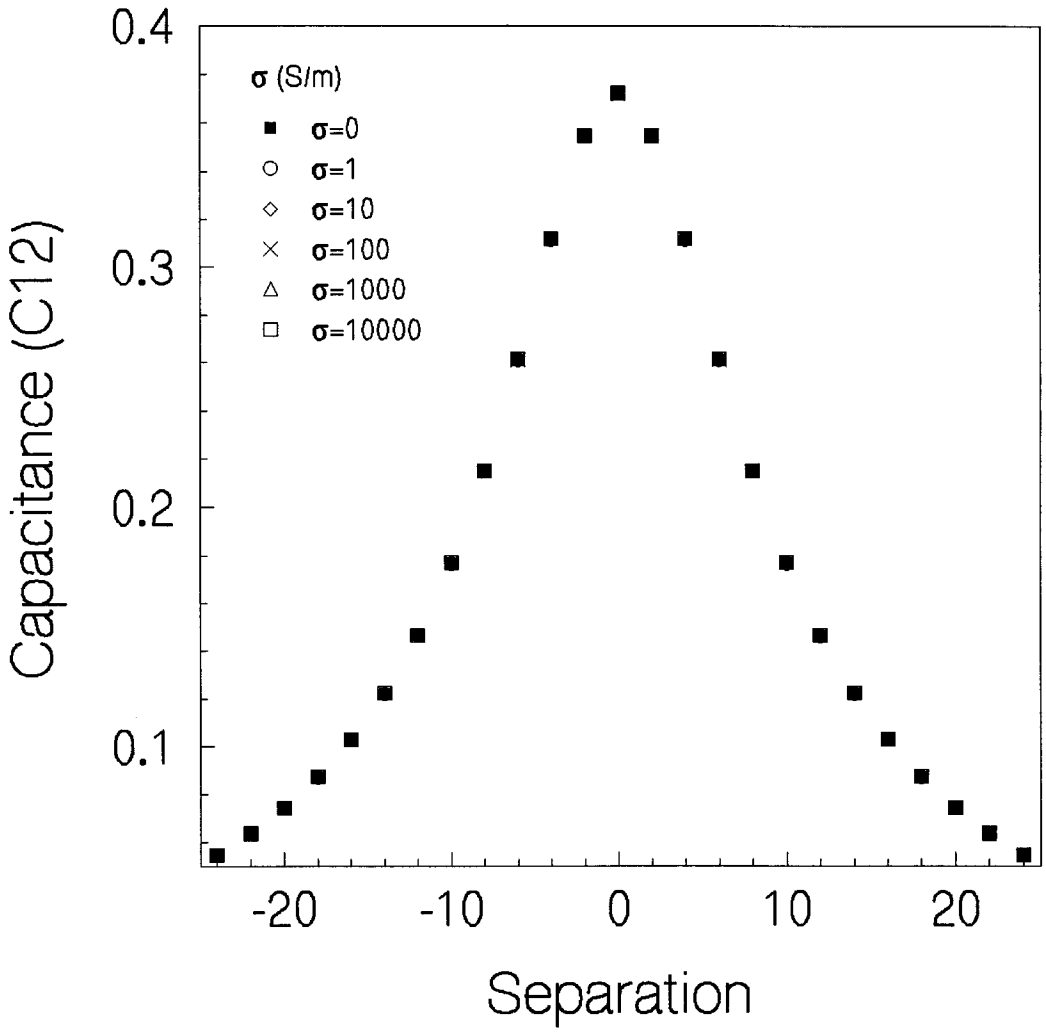

Figure 4.14 Coupling Capacitance vs Separation Distance for varying values of dielectric conductance.

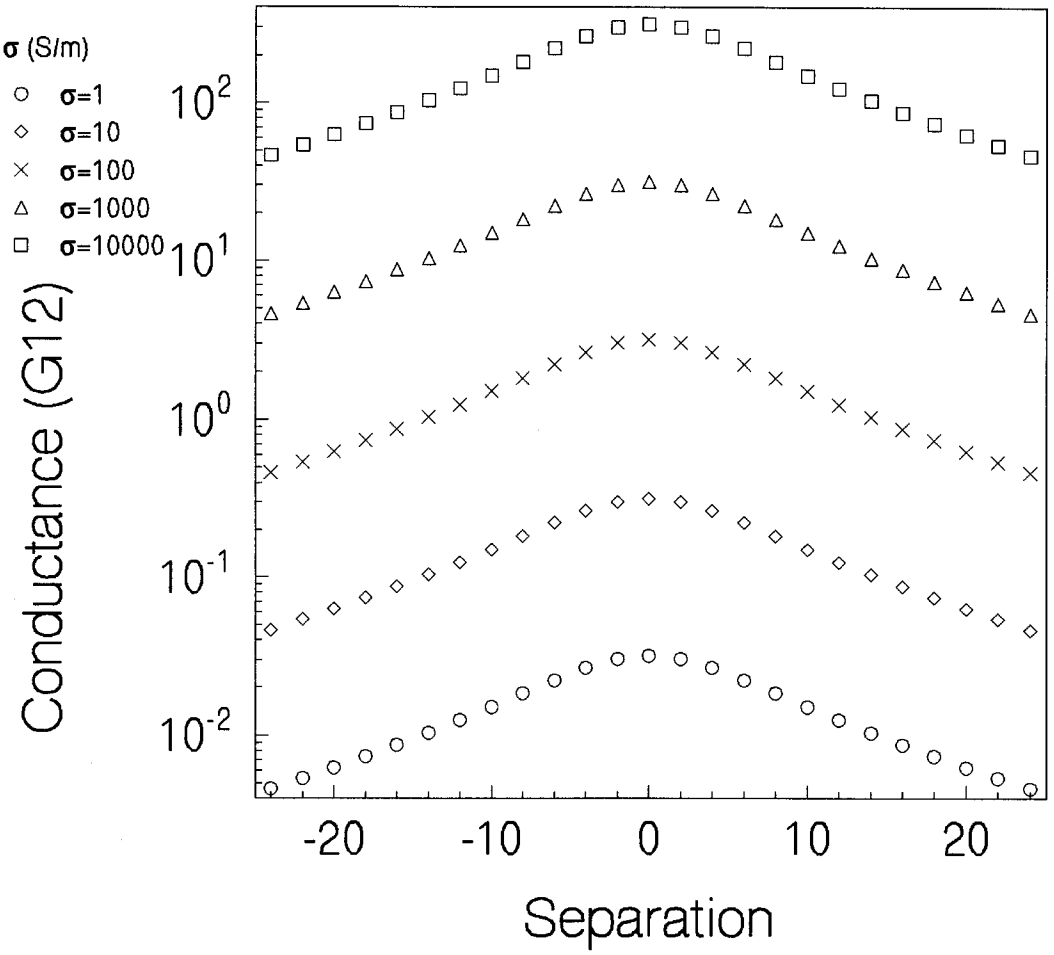

Figure 4.15 Coupling Conductance vs. Separation Distance for varying values of dielectric conductance.

As expected, the coupling capacitance is at a maximum when the two patches are directly on top of one another (d = 0). Also, similar to the first structure, the change in coupling capacitance was less than one

percent for the various values of dielectric conductance.

Figure 4.15 shows how the coupling conductance changes with the change in separation distance as well as with the change in the dielectric conductance. Again, similar to the results for Figure 4.10, the coupling conductance is greatest when the patches are closest together but also varies with the same order of magnitude as the dielectric conductance.

These two analyses show how quickly the circuit parameters can be obtained and how versatile this technique is. In a matter of just a couple of minutes the inputs were entered to analyze the 210 different configurations shown. Once the inputs were set up, the analysis was run and the results obtained in just a few hours. If a third patch were desired or if a new dielectric layer were added, this could be implemented very quickly and easily.

The final analysis which was performed examined the effect of changing the density of the discretization on the processing time and the calculated capacitance. For this analysis, a very simple microstrip structure was used in which the ratio

of the width of the conductor to its height over the ground plane is 2.0 and the relative permittivity of the dielectric medium was set to 2.55, as shown in Figure 4.16.

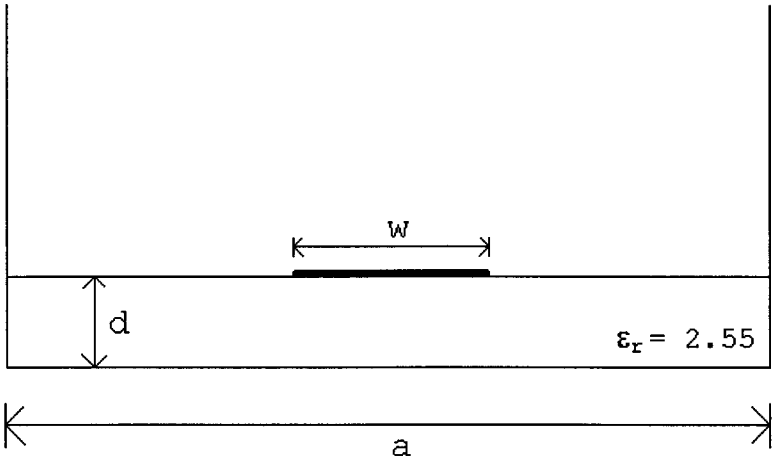

Figure 4.16 Microstip structure

This structure was analyzed for d = 1, 5, 10, 20 and 50. Keeping all other ratios the same, this corresponds to values of W = 2, 10, 20, 40 and 100 and a = 100, 500, 1000, 2000, and 5000. Figure 4.17 shows the results of the simulation time and the value of the capacitance for the different values of d.

d	a	W	C12(pF/m)	CPU time(ms)
1	100	2	73.591	137
5	500	10	76.498	497
10	1000	20	77.135	2,133
20	2000	40	77.471	15,727
50	5000	100	77.652	199,588

Figure 4.17 Capacitance and CPU time vs density of discritization

This structure was analyzed by Pozar[10] for which he obtained the result of C12 = 77.077 pF/m. For the lowest discritization scheme (d=1), these results vary from Pozar's by 4.5%. For the most dense discritization, the difference is .8%. However, the closest result is the one in which d is set to 10. This is probably due to the inaccuracies of Pozar's calculations due to his approximate analysis (he himself indicates that he could obtain more accurate results through some better approximations).

The percent change from the third analysis to the fifth is less than .7% while the percent change from

the first to the second is 3.8%. The density change in both cases is 5 to 1. This shows the diminishing return for increasing the density of the discritization.

Finally, looking at the CPU time used for each analysis shows the problem with increasing the density. In increasing the density five fold from d=1 to d=5, the CPU time increased by approximately three fold (137 ms to 497 ms). In increasing the density five fold from d=10 to d=50, the CPU time increased almost 94 fold (2133 ms to 199588 ms). It has therefore been shown that the greatest gains with increasing the density of the nodes occurs very quickly and any further increases would not typically be justified.

5. SUMMARY AND SUGGESTIONS FOR FURTHER RESEARCH

The quasi-static transmission line parameters of stripline and microstrip planar structures as well as the self- and coupling admittances of planar coupled conducting patches can be easily obtained using the network analog method. This technique discretizes the area of interest to calculate the nodal impedance matrix for the structures. The capacitance matrix can be easily determined from the impedance/admittance matrix.

Overall this technique is very fast and quite accurate. For moderate to small discretization sizes this technique can calculate the quasi-static parameters for complex structures in a relatively small amount of CPU time. This technique can be used to either analyze the structures with high accuracy using a high node count or, perhaps, as a first pass analysis of complicated structures to determine the parameters for a first guess of other more complicated analysis techniques. Higher degrees of accuracy can always be achieved with a more dense discretization scheme, but

usually the cost of the higher accuracy would be a much higher amount of processing time.

This technique, as programmed, is quite useful and its accuracy has been demonstrated. It allows the user to easily set up an analysis and to quickly calculate the quasi-static parameters for complicated structures. However, there are still enhancements to this code which can be made.

First, the change of the code into a faster processing language such as C or perhaps C++, as well as the addition of adding calculations for effective permittivity and input impedance is suggested. This code was written in FORTRAN due to the author's familiarity with the language and FORTRAN's native complex variable type.

In the first paper by Tripathi and Bucolo[2] a technique was presented which would allow for different scaling in the x and y directions. This technique can also be used here, but has not been coded. Perhaps a simple refinement of this technique would be to add the ability to scale the discretizations differently in the different directions.

One of the advantages of this technique is its ability to very easily handle different substrate profiles. One of enhancements made to the two-dimensional version of this technique was the ability to have the program determine various profiles for the permittivity of the substrate, such as a linear, cosine or exponential.

Finally, the ability to handle patches of varying shapes should also be considered. One of the main reasons this was not handled in this program was the complexity of entering such information, and the purpose of this analysis was to determine the accuracy and usefulness of this technique.

BIBLIOGRAPHY

[1] E. Drake *et al.*, "Quick computation of (C) and (L) matrices of generalized multiconductor coplanar waveguide transmission lines," *IEEE Trans. Microwave Theory Tech.*, vol. 42, pp. 2328-2335, December 1994.

[2] M. Tsai and F. De Flaviis, "Modeling planar arbitrarily shaped microstrip elements in multilayered media," *IEEE Trans. Microwave Theory Tech.*, vol. 45, pp. 330-337, March 1997.

[3] T. Kitazawa and T. Itoh, "Propagation characteristics of coplanar-type transmission lines with lossy media," *IEEE Trans. Microwave Theory Tech.*, vol. 39, pp. 1694-1700, October 1991.

[4] M. Alam *et al.*, "Analysis of lossy planar transmission lines using a vector finite element method," *IEEE Trans. Microwave Theory Tech.*, vol. 43, pp. 2466-24??, June 1995.

[5] F. Olyslager *et al.*, "Rigorous analysis of the propagation characteristics of general lossless and lossy multiconductor transmission lines in multilayered media," *IEEE Trans. Microwave Theory Tech.*, vol. 41, pp. 79-??, January 1993.

[6] B. L. Lennarsson, "A network analog method for computing the TEM characteristics of planar transmission lines," *IEEE Trans. Microwave Theory Tech.*, vol. MTT-20, pp. 586-591, September 1972.

[7] V. K. Tripathi and R. J. Bucolo, "A simple network analog approach for the quasi-static characteristics of general lossy, anisotropic, layered structures," *IEEE Trans. Microwave Theory Tech.*, vol. MTT-33, pp. 1458-1464, December 1985.

[8] V. K. Tripathi and R. J. Bucolo, "Analysis and modeling of multilevel parallel and crossing interconnection lines," *IEEE Trans. Electron Devices.*, vol. ED-34, pp. 650-658, March 1987.

[9] R. Collin, "Foundations for Microwave Engineering," McGraw-Hill, New York, 1992.

[10] D. M. Pozar, "Microwave Engineering," Addison-Wesley, Massachusetts, 1990.

[11] B. Bhat and S. K. Koul, "Lumped capacitance, open circuit end effects, and edge-capacitance of microstrip-like transmission lines for microwave and millimeter-wave applications," *IEEE Trans. Microwave Theory Tech.*, vol. 32, pp. 433-439, April 1984.